Intermetallics 19 (2011) 662–665

Contents lists available at ScienceDirect

Intermetallics

journal homepage: www.elsevier.com/locate/intermet

Ca–Mg–Zn–(Ag) bulk metallic glasses prepared by unidirectional quenching

L. Hu [a], B.Y. Liu [a], F. Ye [a,*], B.C. Wei [b], G.L. Chen [a]

[a] State Key Laboratory for Advanced Metals and Materials, University of Science and Technology Beijing, 30 Xueyuan Road, Beijing 100083, People's Republic of China
[b] National Microgravity Laboratory, Institute of Mechanics, Chinese Academy of Sciences, Beijing 100080, People's Republic of China

ARTICLE INFO

Article history:
Received 23 November 2010
Received in revised form
14 December 2010
Accepted 11 January 2011
Available online 21 February 2011

Keywords:
B. Glasses, metallic
B. Thermal properties
C. Rapid solidification processing

ABSTRACT

We fabricated ternary Ca–Mg–Zn and quaternary Ca–Mg–Zn–Ag bulk metallic glasses with diameter of 7 mm by unidirectional quenching into water-cooled Ga–In–Sn liquid alloys. It was suggested that the electromagnetic stirring caused by induction eddy current facilitated the glass formation. Glass forming ability of $Ca_{62.5}Mg_{17.5}Zn_{20-x}Ag_x$ ($x = 0, 1, 3, 5, 7, 9$) system was dependent on Ag content. It was found that in the system the in-situ formed crystalline phases enhanced the second-stage crystallization, whereas there seemed no contribution to the third-stage crystallization.

1. Introduction

Since the first successful formation of metallic glass by rapid solidification of liquid metallic alloy [1], there have been extensive efforts to develop bulk metallic glasses (BMGs) which have excellent glass forming ability (GFA), large supercooled liquid region, and high thermal stability response to crystallization below crystallization temperature (T_x). A number of BMGs have been obtained in Zr-, Ti-, Ln-, Ni-, Cu- and Mg-based systems [2–6]. These metallic alloys provide opportunities for fundamental studies and engineering applications.

Ca-based bulk metallic glasses are a relatively new class of lightweight amorphous alloys which consist of simple alkaline earth metals (Ca and Mg) and late transition metals (*e.g.*, Ag, Cu, Zn and Ni) [7]. They have some unique properties such as low characteristic temperatures, low density, low moduli, and good biocompatibility. The first Ca-based BMGs prepared by conventional copper mold casting were reported by Amiya and Inoue in 2002 [8]. They produced some ternary glasses, $Ca_{67}Mg_{19}Cu_{14}$, $Ca_{57}Mg_{19}Cu_{24}$ and $Ca_{60}Mg_{20}Ag_{20}$, with diameters of 2 mm, 4 mm and 4 mm, respectively, and 7 mm for a quaternary alloy, $Ca_{60}Mg_{20}Ag_{10}Cu_{10}$ [9]. During the following years, a number of Ca–Mg–(Zn, Cu, Al), Ca–Al–Cu, Ca–Mg–Zn–(Cu, Al), Ca–Mg–(Al, Y)–Cu, Ca–Mg–(Al, Y)–Zn-Cu and Ca–Mg–Al–Ag–Cu BMGs with thicknesses up to 10 mm were reported by Senkov et al. [10–13,17]. Park and Kim [14] produced a $Ca_{65}Mg_{15}Zn_{20}$ bulk glassy alloy by casting into cone-shaped copper mold in air atmosphere with a diameter up to 15 mm. Laws and Ferry [15] reported the $Ca_{65}Mg_{15}Zn_{20}$ glass of dimensions 3.15 mm × 7 mm × 125 mm prepared by low pressure die-casting technique. All of these Ca-based BMGs can be described by the formula [16]:

$$Ca_A\,(Y, Ln)_B\,(Mg, Sn)_C\,(Al, Ag, Ga, Zn)_D\,(Cu, Ni)_E$$

where $A = 0.40–0.70$; $B = 0–0.25$; $C = 0–0.25$; $D = 0–0.35$; $E = 0–0.35$, $B + C + D \geq 0.05$ and $A + B + C + D + E = 1$.

In present work, unidirectional quenching method which could maintain the melt motion behavior until it was frozen was employed to produce Ca-based BMGs. Ag as one biophile metal was introduced into Ca-based BMGs which has potential prospects on artificial bones, because Ag ions and compounds can kill and inhibit virus and bacteria. Dependence of glass forming ability of $Ca_{62.5}Mg_{17.5}Zn_{20-x}Ag_x$ ($x = 0, 1, 3, 5, 7, 9$) alloy on the content of Ag was studied.

2. Experimental procedures

The melting temperature (T_m) of all constituent elements is below 1273 K, among which Zn has the lowest T_m (693 K) and the highest volatility. Ingots of master alloys were prepared by induction melting of mixtures of pure elements (purity > 99.9 wt.%) in silica tubes in an argon atmosphere. A certain amount of ingots were placed into alumina tube with an internal diameter of 7 mm and a wall thickness of 0.5 mm. The ingots were heated to liquid phase by high frequency induction, before unidirectional quenching was carried out. Finally, the melt was quenched into a water-

* Corresponding author. Tel.: +86 10 6233 3899; fax: +86 10 6233 2508.
E-mail address: yefeng@skl.ustb.edu.cn (F. Ye).

0966-9795/$ – see front matter © 2011 Elsevier Ltd. All rights reserved.
doi:10.1016/j.intermet.2011.01.003

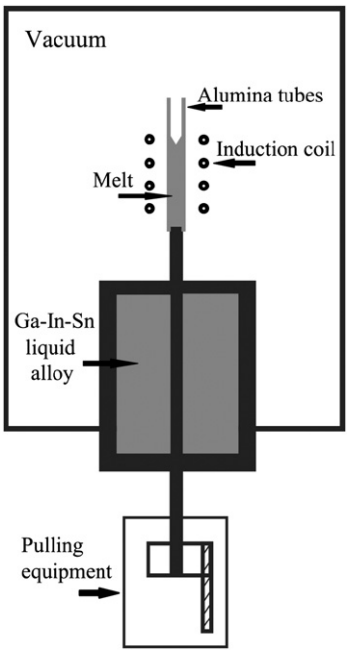

Fig. 1. A schematic representation of unidirectional quenching unit for the production of Ca-based bulk metallic glasses.

cooled Ga–In–Sn liquid alloy. Fig. 1 is a schematic diagram of induction-heated unidirectional quenching equipment. X-ray diffractometer (Rigaku D/MAX—RB) using Cu Kα radiation was employed for identification of amorphous nature of as-prepared samples. Thermal analysis associated with glass transition, supercooled liquid region, crystallizations of the Ca-based alloy samples were performed in a NetzschSTA449C differential-scanning calorimeter with a constant heating rate of 20 K/min under an argon atmosphere. The weight of samples used for DSC was about 10–20 mg.

3. Results and discussion

Fig. 2 shows the X-ray diffraction patterns of all Ca-based alloys prepared by unidirectional quenching. Table 1 gives all alloy compositions. The alloys from #1 to #5 show only a broad diffraction peak in the range of 25–40°, and no diffraction peaks

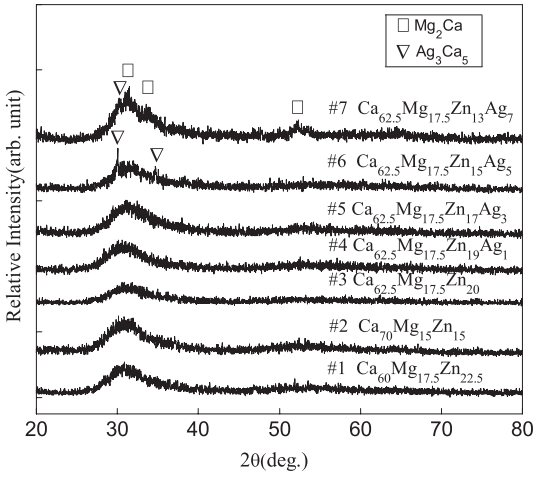

Fig. 2. X-ray diffraction patterns of as-quenched samples of Ca–Mg–Zn–(Ag) alloys.

corresponding to crystalline phases are detected, indicating the fully amorphous state of these alloys. Low intensity sharp peaks from crystalline phases, together with a broad diffraction peak, are characteristics of X-ray diffraction patterns from the alloys #6 and #7, indicating these alloys are partially crystalline. Representative differential-scanning calorimeter (DSC) curves of the as-quenched alloys are given in Fig. 3. An endothermic reaction corresponding to the glass transition and the supercooled liquid region are typical of all alloys, followed by exothermic reactions due to crystallization. The glass transition temperature (T_g), crystallization temperature (T_{x1}) and the onset temperature of melting endotherm (T_m) are marked by arrows in the DSC traces. There are almost three distinct crystallization peaks for fully amorphous Ca-based alloys. In this work, we define T_{x1}, T_{x2} and T_{x3} as the onset temperatures of first-stage, second-stage and third-stage crystallization, respectively. The state after quenching, characteristic temperatures (T_g, T_x, T_m, supercooled liquid range $\Delta T_x = T_{x1} - T_g$, reduced glass transition temperature $T_{rg} = T_g/T_m$) of all seven alloys are shown in Table 1.

For the ternary alloys, $Ca_{60}Mg_{17.5}Zn_{22.5}$, $Ca_{62.5}Mg_{17.5}Zn_{20}$ and $Ca_{70}Mg_{15}Zn_{15}$, they are fully amorphous when the diameter is 7 mm. It indicates that the critical diameter for formation of a single glassy state of the three alloys is larger than 7 mm. T_g decreases from 380K to 376K, T_{x1} decreases from 423 K to 411 K and T_{x3} also has the decreasing tendency from 490 K to 483 K, when the concentration of Ca increases from 60% to 70% and the concentrations of Mg and Zn decrease. The feature that characteristic temperatures vary with the concentrations of constituent elements also can be seen in other Ca–Mg–Zn compositions [13].

Senkov draws a trapezoid-like area in the liquidus projection of Ca–Mg–Zn ternary phase diagram according to the glass forming ability [16]. In his opinion, better glass forming alloys are located in the center while poorer glass formers are located at the edges of this region. $Ca_{60}Mg_{17.5}Zn_{22.5}$ and $Ca_{62.5}Mg_{17.5}Zn_{20}$ are located in the center and their glass forming size is larger than 7 mm. This is in accordance with his opinion. For $Ca_{70}Mg_{15}Zn_{15}$ glass, it is located at the edge of the area, but its critical size is sufficiently bulk, larger than 7 mm, too. We suppose it is because of the unique characteristics of our preparation methods.

In the unidirectional quenching, the melt was heated by electromagnetic induction eddy current which acted as a nonintrusive stirring device and stirred liquid strongly [18]. The melt was whirled continuously until it was frozen completely which can be verified by the apparent swirl-shaped top of each as-quenched sample (see the inset of Fig. 4). As the electromagnetic stirring is to the grain refinement of conventional crystal materials, we consider that the forceful stirring facilitates the glass formation here. To confirm the supposition, the comparison experiments are performed as follows.

We selected $Ca_{60}Mg_{20}Zn_{20}$ as the master alloy which has the glass forming critical diameter up to 4 mm [16]. Graphite sleeve was placed between the alumina tube and induction coil to shield the induction magnetic field and obstruct electromagnetic stirring. In this case, the melt would be heated by thermal radiation of graphite. The unidirectional quenching was performed without (sample a) and with graphite sleeve (sample b), respectively. Fig. 4 gives XRD patterns of the two samples with diameter of 7 mm. One single broad diffraction peak indicated the amorphous nature of sample (a) prepared with electromagnetic stirring. The XRD pattern of sample (b) prepared without electromagnetic stirring shows numerous sharp peaks corresponding to crystalline phases. The inset of Fig. 4 displays the top and cross-section of the two samples. Sample (a) has a swirl-shaped top and shiny cross-section which is typical of BMGs. The top of sample (b) is irregular and the cross-section is intensively dim.

Table 1
Compositional range, state after quenching (A represents amorphous, C represents crystal, the value of percentages are the volume fraction of crystalline phases in Ca-based alloys), glass transition temperature (T_g), crystallization temperature (T_{x1}, T_{x2}, T_{x3}), onset temperature of melting endotherm (T_m), supercooled liquid range $\Delta T_x = T_{x1} - T_g$, reduced glass transition temperature $T_{rg} = T_g/T_m$ for all Ca-based alloys.

Alloy no.	Alloy	State after quenching	T_g(K)	T_{x1}(K)	T_{x2}(K)	T_{x3}(K)	ΔT_x(K)	T_m(K)	T_{rg}
1	$Ca_{60}Mg_{17.5}Zn_{22.5}$	A	380	423		490	43	605	0.628
2	$Ca_{70}Mg_{15}Zn_{15}$	A	376	411	447	483	35	608.5	0.618
3	$Ca_{62.5}Mg_{17.5}Zn_{20}$	A	378	413	445	490	35	603	0.627
4	$Ca_{62.5}Mg_{17.5}Zn_{19}Ag_1$	A	376	407	441	485	31	605.5	0.621
5	$Ca_{62.5}Mg_{17.5}Zn_{17}Ag_3$	A	378	410	444	489	32	611.5	0.618
6	$Ca_{62.5}Mg_{17.5}Zn_{15}Ag_5$	A + C (11%)	378	419	442	497	41	615	0.615
7	$Ca_{62.5}Mg_{17.5}Zn_{13}Ag_7$	A + C (20%)	379	416		497	37	621	0.610

Two explanations for the formation of bulk $Ca_{70}Mg_{15}Zn_{15}$ and $Ca_{60}Mg_{20}Zn_{20}$ glasses prepared with electromagnetic stirring are proposed.

1. Difficulty in nucleating
   Owing to the intensive whirling, the liquid was always homogeneous and nucleation was greatly difficult [19]. The inhibition of nucleation benefited the transformation from homogeneous liquid to glassy state at the large cooling rate.

2. Suppression of growing
   Even though the nuclei formed occasionally and grew, but the powerful stirring would break the growing nuclei. These nuclei or embryo had no time to grow up and were solidified to glass.

The glass forming ability of $Ca_{62.5}Mg_{17.5}Zn_{20-x}Ag_x$ ($x = 0, 1, 3, 5, 7, 9$) system ($x = 9$ is not shown here and it is fully crystalline) was dependent on the content of Ag. From the XRD diffraction patterns, the formation of a single glassy phase was found when $x = 0, 1, 3$. Crystalline phases were detected when $x = 5$. We evaluated the volume fraction of the crystalline phases by analyzing the contrast from SEM images ($\lambda = S^{crystalline\ phases}/S^{total}$, S means area) and calculating crystallization enthalpy from DSC curves ($\lambda = \Delta H_x^{compound}/\Delta H_x^{fully\ amorphous}$). When x changes from 5 to 7 and 9, λ increases from 11% to 20% and 100%. Fig. 5 shows the relationship between volume fraction of crystalline phases in the as-quenched Ca-based alloys and Ag content.

Table 1 shows that, for $Ca_{62.5}Mg_{17.5}Zn_{20-x}Ag_x$ ($x = 0, 1, 3, 5, 7, 9$) alloys, T_g is almost unchanged and T_m increases as x increases, but T_{x1} varies randomly with x. In spite of the formation of crystalline phases, the supercooled liquid region ΔT_x of composite $Ca_{62.5}Mg_{17.5}Zn_{20-x}Ag_x$ ($x = 5, 7$) is larger than amorphous $Ca_{62.5}Mg_{17.5}Zn_{20-x}Ag_x$ ($x = 0, 1, 3$). However, reduced glass transition temperature T_{rg} exhibits good correlation with GFA evaluated by volume fraction of crystalline phases [20]. In the DSC curves, we can see migration of the three crystallization peaks as the growth of Ag content. In the fully amorphous state of $Ca_{62.5}Mg_{17.5}Zn_{20-x}Ag_x$ ($x = 0, 1, 3$) three distinct crystallization peaks can be distinguished. With the formation of crystalline phases ($x = 5, 7$) the second-stage crystallization peak gradually approaches the first-stage crystallization peak (see the dash line in Fig. 3), but the third-stage one almost does not move. Temperature interval of the onset temperature of different stage crystallization ($\Delta T_{x12} = T_{x2} - T_{x1}$, $\Delta T_{x13} = T_{x3} - T_{x1}$) as a function of Ag content for $Ca_{62.5}Mg_{17.5}Zn_{20-x}Ag_x$ ($x = 0, 1, 3, 5, 7$) alloys are given in Fig. 5. As can be seen from Fig. 5, variation tendency of ΔT_{x12} in the as-quenched Ca-based alloys is opposite to that of volume fraction of the

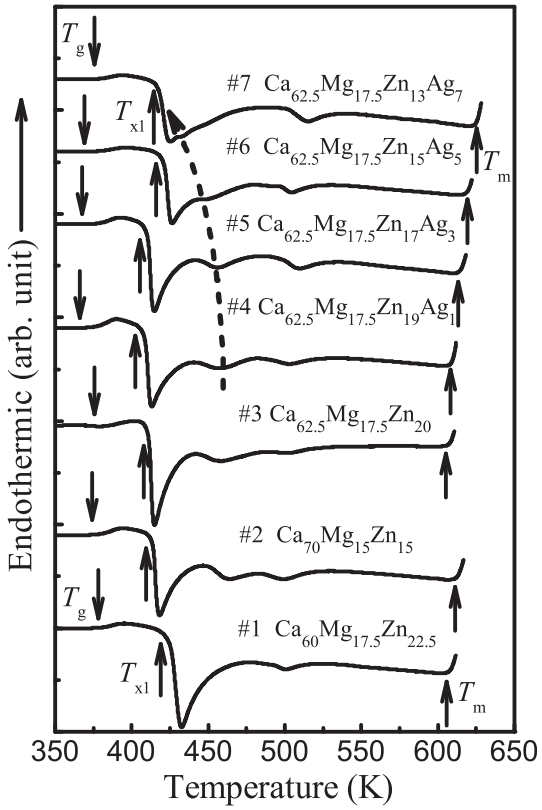

Fig. 3. DSC curves of as-quenched Ca–Mg–Zn–(Ag) alloys. The heating rate is 20 K/min. The glass transition temperature (T_g), crystallization temperature (T_{x1}) and the onset temperature of melting endotherm (T_m) are marked by arrows in the traces. The dash line represents the migration tendency of second-stage crystallization peak.

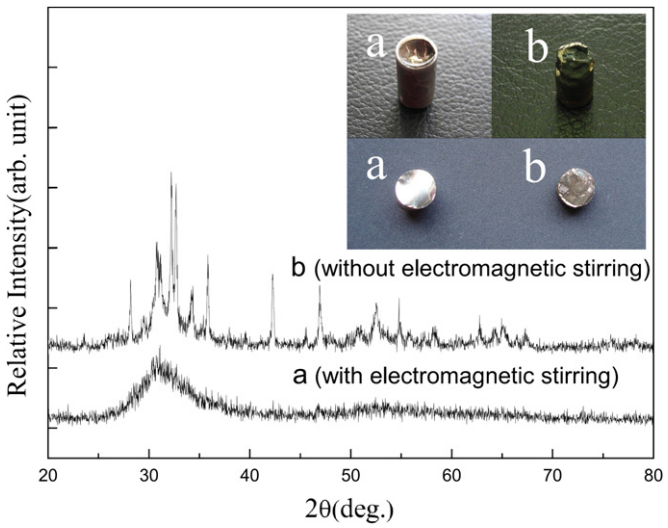

Fig. 4. X-ray diffraction patterns of the samples prepared without and with electromagnetic stirring. The inset displays the top and cross-section of the two samples, the dark part of top is because of the solidification of volatile.

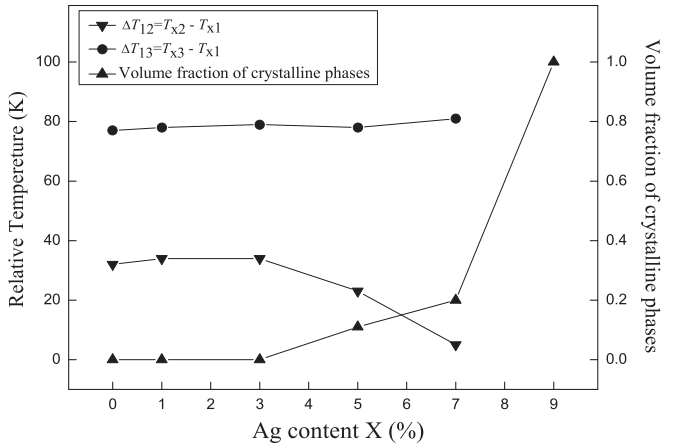

Fig. 5. The relation between x (Ag content) and volume fraction of crystalline phases for $Ca_{62.5}Mg_{17.5}Zn_{20-x}Ag_x$ (x = 0, 1, 3, 5, 7, 9) alloys and temperature interval of the onset temperatures of different stage crystallization ($\Delta T_{x12} = T_{x2}-T_{x1}$, $\Delta T_{x13} = T_{x3}-T_{x1}$) as a function of Ag content.

crystalline phases. When $x = 5$, the second-stage crystallization peak move backward a little. ΔT_{x12} decreases to 23 K, but ΔT_{x13} does not deviate from the formers. When $x = 7$, the second-stage crystallization peak and the first-stage one overlaps, namely, the first-stage crystallization starts firstly and then the first-stage and second-stage ones proceed simultaneously. But ΔT_{x13} still does not deviate. We consider that the existence of in-situ crystalline phases in the amorphous matrix promotes the second-stage crystallization, but there seems no contribution to the third-stage crystallization. The crystallization process of Ca-based BMGs is an interesting issue and requires further investigations.

4. Conclusion

1. Ca–Mg–Zn–(Ag) BMGs were fabricated in cylindrical shape with diameters of 7 mm by unidirectional quenching. The unidirectional quenching method can be applied to BMGs formation extensively, especially for low melting point alloy which is difficult to be formed by conventional arc-melting copper mold casting.
2. The positive effect of electromagnetic stirring on the formation of the glassy state is understandable, but details need further studies.
3. Glass forming ability of $Ca_{62.5}Mg_{17.5}Zn_{20-x}Ag_x$ ($x = 0, 1, 3, 5, 7, 9$) system was dependent on Ag content. The in-situ formed crystalline phases enhance the second-stage crystallization, but there seems no contribution to the third-stage crystallization.

Acknowledgments

The authors gratefully acknowledge the financial support from the Fundamental Research Funds for the Central Universities (FRF-TP-09-026B) and Ph.D. Programs Foundation of Ministry of Education of China (20100006110013).

References

[1] Klement W, Willens R, Duwez P. Nature 1960;187:869–70.
[2] Inoue A, Zhang T, Masumoto T. Mater Trans 1990;31:177–83.
[3] Peker A, Johnson WL. Appl Phys Lett 1993;63:2342–4.
[4] Yim HC, Xu DH, Johnson WL. Appl Phys Lett 2003;82:1030–2.
[5] Inoue A, Nakamura T, Nishiyama N, Masumoto T. Mater Trans 1992;33:937–45.
[6] Inoue A. Acta Mater 2000;48:279–306.
[7] Takeuchi A, Inoue A. Mater Trans 2005;46:2817–9.
[8] Amiya K, Inoue A. Mater Trans 2002;43:81–4.
[9] Amiya K, Inoue A. Mater Trans 2002;43:2578–81.
[10] Senkov ON, Scott JM. Scripta Mater 2004;50:449–52.
[11] Senkov ON, Scott JM. Mater Lett 2004;58:1375–8.
[12] Senkov ON, Scott JM, Miracle DB. J Alloys Compd 2006;424:394–9.
[13] Senkov ON, Miracle DB, Keppens V, Liaw PK. Metall Mater Trans A 2008;39:1888–900.
[14] Park ES, Kim DH. J Mater Res 2004;19:685–8.
[15] Laws KJ, Gun B, Ferry M. Mater Sci Eng A 2008;475:348–54.
[16] Senkov ON, Miracle DB, Scott JM. Intermetallics 2006;14:1055–60.
[17] Senkov ON, Scott JM. J Non-Cryst Solids 2005;351:3087–94.
[18] Moffatt HK. Phys Fluids A 1991;3:1336–43.
[19] Tamura T, Amiya K, Rachmat RS, Mizutani Y, Miwa K. Nat Mater 2005;4:289–92.
[20] Park ES, Kim WT, Kim DH. Mater Sci Forum 2005;475–479:3415–8.